

Ophthalmic Diseases Classification Based on YOLOv8

Ahmed Tuama Khalaf¹, Salwa Khalid Abdulateef^{2*}

^{1,2} Computer Science Department Computer Science and Mathematics College, Tikrit University, Tikrit, Iraq
Email: ¹ahmed.t.khalaf@st.tu.edu.iq, ²Khalid.salwa@tu.edu.iq

*Corresponding Author

Abstract—With the rising prevalence of retinal diseases, identifying eye diseases at an early stage is crucial for effective treatment and prevention of irreversible blindness. But Ophthalmologists face challenges in detecting subtle symptoms that may indicate the presence of a disease before it progresses to an advanced stage. Among these challenges, eye diseases can present with a wide range of symptoms, and some conditions may share similar signs. To solve these difficulties, in the research proposed YOLOV8 (You Only Look Once) Lightweight Self-Attention model to classify seven different retinal diseases. In this regard, the dataset that have been used in this study contains 5787 images from three different sources (Roboflow, Kaggle and Medical Clinics) were included in the seven classes of Glaucoma, Age-related Macular Degeneration (AMD), Cataract, Diabetic retinopathy (DR), and Retinal Vein Occlusion, which comprises of Branch Retinal Vein Occlusion (BRVO) and Central Retinal Occlusion (CRVO) and normal. As a results, the model has proven excellent performance in its classification ability. Boasting an average classification accuracy of 94% across the seven disease with precision 96.2%, recall 96.6% and f1 score was 96.3%. At the time of training it was 0.6 Hours (H). When compared with Resnet50, VGG16 results underscore the model's superior performance in precision and computational efficiency compared. The algorithm's evaluation reveals its superiority when compared to earlier pertinent research, making it a trustworthy method for classifying retinal illnesses.

Keywords—Ophthalmic Disease; Deep Learning; Fundus Image; Yolov8; Resnet50; Vgg16.

I. INTRODUCTION

According to the World Health Organization (WHO), Nearly 2.2 billion people worldwide suffer with vision impairment [1]-[3]. Early modification in the retina are influenced by a variety of variables, such as unfavorable environmental conditions, including aging, a high-carbohydrate diet, systemic diseases, including hyperglycemia, hyperlipidemia, and hypertension [4][5]. Around the world, there are 300 million people with vision impairment and 45 million people who are blind, with more than 90 percent of them living in developing nations. These numbers are increasing by the day, particularly among individuals over the age of 75 [6]. Diabetes is a worldwide problem. Diabetes is one of the fastest-growing diseases in recent times, but it is especially prevalent in Indian society [7]-[9]. Diabetes affects 422 million individuals globally. According to the Lancet report, China, India, and the US have the highest number of diabetics [10]-[14]. Closely related in diabetic retinopathy (loss of vision) a crucial eye ailment that causes in loss. In general People with a long history of

diabetes are more likely to be afflicted with this condition, and one out of every 10 will have vision loss [15]-[18]. Diabetic retinopathy is expected to occur from 126.6 million to 191.1 million by 2030. Following diabetic retinopathy, retinal vein occlusion (RVO) can be specified as the second most prevalent retinal vascular disease [19][20]. About 16.4 million individuals are expected to be affected by RVO globally, with a prevalence of 2.1% in the general population over 40 [21]-[25]. RVO consists of two sections as central and branch (CRVO and BRVO). CRVO includes superficial or deep retinal hemorrhages (HEs) that are dispersed along the vein at the lamina cribrosa [26]-[29]. Vascular injury, Virchow's triad comprises hypercoagulability, stasis, and vessel damage. thrombogenesis—are assumed to underpin the pathogenesis of CRVO [30]-[34]. BRVO BRVO is the second most prevalent retinal vascular condition, after diabetic retinopathy, is the blockage of a retinal vein branch at an arteriovenous crossing [35]-[37]. It is believed that the compression of the vein causes turbulent blood flow, which triggers the formation of thrombus. Thrombosis could cause engorged veins with varying degrees of retinal non-perfusion. if RVO is not treated in a timely manner, it can develop to major problems and cause serious visual impairment [38][39]. A cataract is defined as a clouding of the lens of the eye that impairs vision. One of the main causes of blindness is cataracts [40][41]. Up to 191 million individuals might be affected by blindness, of which 32.4 million now suffer. It is projected that 40 million people globally would be blind due to cataracts by the year 2025 [42][43]. Glaucoma, sometimes known as "the silent thief of sight," is the world's second largest cause of blindness. This condition affects more than 60 million individuals worldwide, and by 2020, that figure is predicted to climb to 79.6 million. Glaucoma is an irreversible eye ailment., it needs to be identified and treated right away [44]. One factor affecting macula safety is age-related macular degeneration (AMD), which is prevalent in the elderly population [45]. Worldwide, AMD is the fourth most common cause of blindness. It was predicted that 196 million people worldwide will be infected with AMD by 2020, increasing to 288 million by 2040 [46]. DL has demonstrated notable benefits in a range of real-world applications lately [47][48]. Various attempts were made to use retinal fundus images and DL approaches to identify retinal eye disorders. Classifying multi-class retinal eye diseases is still a difficult task, despite the fact that DL approaches in machine learning (ML) have produced excellent results in binary classification tasks that distinguish between healthy and diseased retinal fundus images [49][50].



Despite the effectiveness of CNN-based approaches. Previous studies utilizing classic CNN models such as Resnet50 or VGG16 have faced significant difficulty in classifying eye disorders. These algorithms are insufficient in terms of accuracy, storage space, and speed due to complex mathematical operations. Although accuracy and computational efficiency are considered among the most prominent classification techniques, these obstacles are in addition to them. There is no complete database that encompasses all of the diseases that are thought to be among the most common causes of blindness; in fact, earlier research were confined to classify them into two, three, or four categories. In our research article, we worked hard to tackle the issues utilizing a new, lightweight model (YOLOv8). That outperforms earlier systems in terms of performance and accuracy. In addition, we classified six disease categories that may lead to blindness, with the seventh health condition we compiled one database from three sources. For the two categories (BRVO and CRVO). We collected it locally because it is not available or in very few pictures, as it is considered the second most prevalent retinal vascular condition, after diabetic retinopathy. The Fig. 1 shows the statistical rates of Ophthalmic diseases in the world.

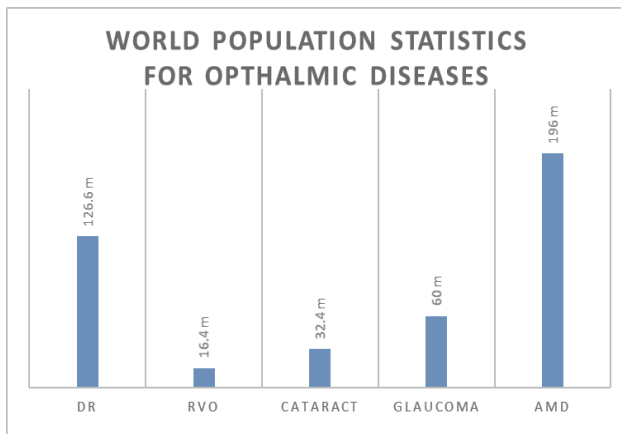


Fig. 1. The statistical rates of Ophthalmic diseases in the world

II. YOLOV8

YOLO (You Only Look Once), a popular detection of objects and image segmentation approach, was created by Joseph Redmon and Ali Farhadi. YOLO, which was launched in 2015, soon garnered popularity due to its great speed and accuracy [51]. Ultralytics' most recent YOLO iteration is known as YOLOv8 [52]. With new features and upgrades that enhance performance, efficiency, and flexibility, YOLOv8 is a state-of-the-art (SOTA) model that performs a variety of vision AI tasks, including segmentation, detection, tracking, pose estimation, and classification. It builds upon the success of previous versions [53]-[55]. YOLOv8 Architecture Explained in Fig. 1. The YOLOv5 team release YOLOv8[56] in January 2023. The primary improvements are as follows:

A. The YOLOv8 Backbone

CSPDraknet-53 in contrast with YOLOv5, YOLOv8's C3 module has been changed with the C2f. Module with more gradient flow. Channel numbers are modified for different scale models to obtain more lightweight. YOLOv8 still uses the SPPF module from YOLOv5.

B. Head

The Head segment has two significant improvements over YOLOv5. The current Decoupled-Head technique separates classification and detection, thereby replacing the prior method. Second, it has changed from anchor-based to anchor-free.

C. Loss

YOLOv8 replaces previously used IOU matching or unilateral ratio distribution methods with the Task-Aligned Assigner positive and negative sample matching method. Furthermore, YOLOv8 incorporates Distribution Focal Loss (DFL) [57]. Data augmentation could enhance model performance. However, introducing mosaic augmentation. Training may have detrimental repercussions. YOLOv8 improves accuracy by turning off Mosaic augmentation in the latest 10 epochs. YOLOv8 offers multiple size models (N, S, M, L, and X) to accommodate various scenarios.

On the MS COCO dataset test-dev 2017, YOLOv8X achieved an AP of 53.9% with 283 FPS using NVIDIA Tesla A100 and TensorRT [58]. YOLOv8 architecture Explains in Fig. 2.

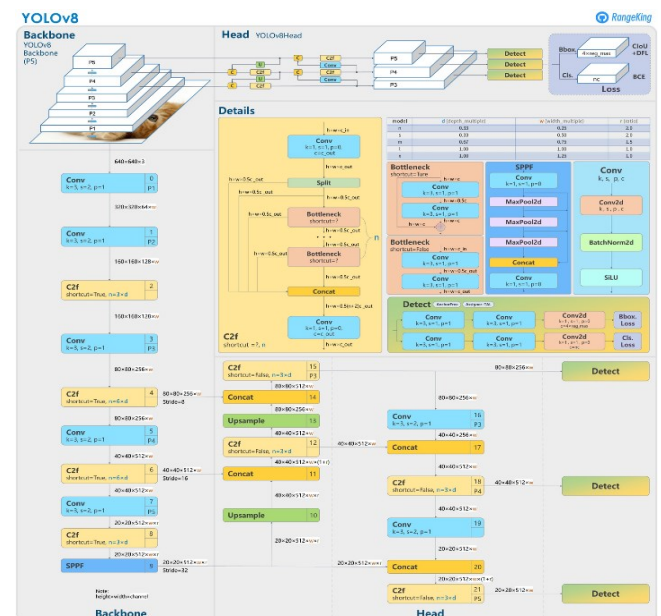


Fig. 2. YOLOv8 architecture

III. LITERATURE SURVEY

Various research works have been conducted on the stages of classifying eye diseases in the specific section based on their importance and which increase the risk of blindness. Researchers have proposed different models for classifying these diseases. Many authors have done so. They have worked and obtained good results. S. Dash, et al. (2023) [59], based on CNN layers, the suggested model vgg16 is intended to identify the five main retinal problems from a limited number of fundus images. After that, real-time fundus images that were collected as pictures were used to cross-validate the model. The accuracy regarding the suggested system is 92.99% on average. E. Abitbol et al. (2022) [60], the purpose of the presented work was to evaluate the capability of a DL model, namely the DenseNet121 network, to discriminate

between diabetic retinopathy (DR), retinal vein occlusions (RVOs), sickle cell retinopathy (SCR), and normal eyes with the use of ultra-widefield color fundus photography (UWF-CFP). The model has been used on a dataset from Creteil University Hospital that included 224 images from each of the four disease categories. Following 10 epochs, findings have shown an overall 88.40% accuracy and their AUC has been 88.50%. W. Xu, et al.'s 2022 research [61] focused upon the development of DL-based intelligent system as well as the exploration of its application to classification and diagnoses of RVO through using fundus images. 501 fundus images of both RVO patients and healthy eyes have been utilized for testing and model training. Using a fundus disease framework, referred to as ResNet18, the images were initially divided into four groups for this study. Fifty epochs in total have been trained. One of the three attention mechanisms—squeeze and excitation network (SENet), coordination attention (CA), or convolutional block attention module (CBAM)—produced a high accuracy of more than 94% in each of the four groups. X. Luo, et al. in 2021[2], utilizing a real-world ophthalmic dataset regarding 5,000 patients in China with retinal fundus images as well as clinical data, they identified a few eye conditions, including cataracts, glaucoma, and age-related macular degeneration (AMD), called OIA-ODIR image for three different disease and healthy. Adaptive histogram equalization is referred to as AHE. Set the dropout rate to 0.3 and the input size to 300×300. Two baseline techniques are EfficientNet-B3 with binary crossentropy loss, BCL-EfficientNet-B3 and FL-EfficientNet-B3. They suggest using the FCL-EfficientNet-B3 model. Between AMD and normal, glaucoma and normal, and cataract and normal, the model's accuracy was 90.08%, 84.78%, and 99.38%, respectively. R. Sarki et al. (2021) [49], this study introduced a new CNN model that can classify Diabetic Eye Disease (DED) into various groups. 1,748 data points, the Messidor, DRISHTI-GS, Messidor-2, and Kaggle cataract databases, Retinal fundus images were enhanced with contrast by using mathematical morphology. By using the right model parameters and enhancing the quality of the training images. The proposed model in RMSprop optimizer yielded the maximum sensitivity and specificity. The suggested CNN model achieved 81% accuracy in the test dataset. In 2023, T. Babaqi, et al [62] the study aimed to distinguish between normal eyes and those with diabetic retinopathy, cataracts, or glaucoma. The following resources were used to acquire information about using CNN and transfer learning for multi-class classification. The dataset contains approximately 4200 colored photos of normal eyes, cataracts, diabetic retinopathy, and glaucoma. The images were resized from 512×512 to 224×224. The suggested transfer learning approach is based on a pre-trained EfficientNet CNN architecture model, which obtained 84% accuracy. C. Wan et al. (2022) [63] employed DL approaches to screen RVO using swin transformers. They apply label smoothing, a regularization technique that employs one-hot noise addition to suppress overfitting. This results in the division of fundus images into four categories: MRVO, normal, BRVO, and CRVO. In the case when utilizing Swin Transformer, mainly focus on two things: the model's high accuracy during training and its strong generalization ability

during application; The study's dataset has 805 fundus images in total, and the model's accuracy was 98.25%.

IV. RESEARCH METHODOLOGY

This section presents the framework Ophthalmic Diseases classification as illustrated in Fig. 1. The collected data are fed into a preprocessing block in subsection A Subsequently, we present the augmentation of data in subsection B followed by the proposed model in subsection C Subsection D contains the suggested model's evaluation metrics. Fig. 3 shows Research Methodology steps.

A. Image Acquisition and Preprocessing

Three different datasets, namely Roboflow, Kaggle, and Medical Clinics were used for getting fundus images. The main features of the datasets are given below.

- Roboflow dataset

The Roboflow dataset has a contain 4215 fundus images for each (DR, Glaucoma, Normal, Cataract). All 4215 images are in JPG format resolution of the images is 224×224 with eight bits per color we used 4215 images with 80% being used for training and 20% for testing.

- Kaggle dataset

The Roboflow dataset has a contain 511 fundus images for AMD are in JPG format resolution of the images is 300×300 with eight bits per color we used 511 images with 80% being used for training and 20% for testing.

- Medical Clinics dataset

The Medical Clinics dataset has a contain 1061 fundus images Which was obtained from Salahuddin, Iraq for each CRVO AND BRVO Two medical experts diagnosed the risk of RVO These images originated from the optical coherence tomography (OCT) device, capturing eye disease images without surgical procedures. All of images in JPG format resolution of the images is 1200×1200, 600×600 with eight bits per color we used 1061 images with 80% being used for training and 20% for testing.

- Preprocessing

All of the fundus images have been pre-processed to have a set size of 224 by 224. A total of 5787 images made up the combined dataset, called Ophthalmic Data, which was split into 20% for testing and 80% for training. Table I displays the data divided into testing and training. Fig. 4 It shows a group of fundus image called Ophthalmic Data. One of the most important features used in Yolov8 during training is that some improvements are made to the images automatically, such as: contrast was (0.6, 1.4), saturation (0.304, 1.7), hue was (-0.015, 0.015)].

TABLE I. DIVIDE THE DATA INTO TRAINING AND TESTING

Classes	Data set	No. of Image	Train	Test
Cataract	Roboflow	4215	838	198
Glaucoma			791	216
Normal			866	208
DR			878	220
CRVO	Clinical Medicine	1061	410	103
BRVO			438	110
AMD	Kaggle	511	408	103

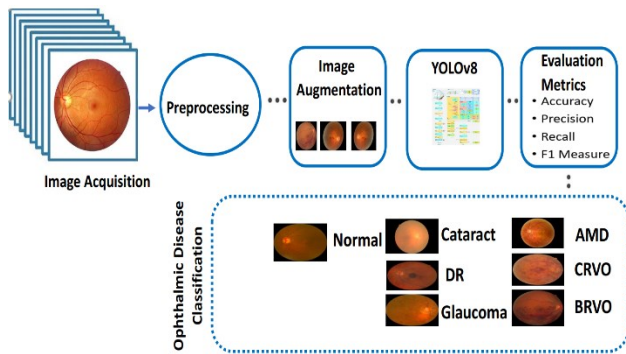


Fig. 3. Research methodology

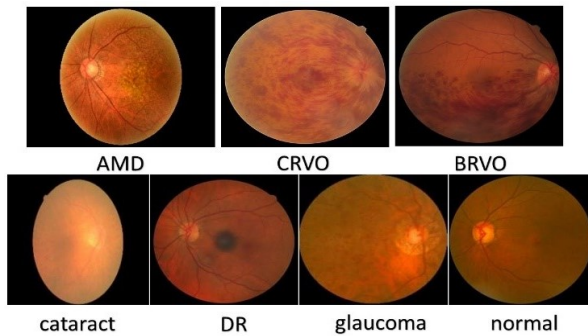


Fig. 4. Retinal fundus color image of different condition

B. Image Augmentation

After dividing the data into 80% training and 20% testing, we notice AMD, CRVO, and BRVO. The sum of all training data was significantly lower than the other categories. Because of the imbalance between the aforementioned disease categories. As a result, it will cause the following issues: Models may become biased toward predicting the majority class in order to obtain higher accuracy. Poor Generalization: Models may struggle to generalize effectively to minority classes, resulting in inferior performance in such classes. To avoid these complications. We attempted as much as possible to balance all categories, therefore we augmented the data for each AMD, CRVO, BRVO. Only for training data. Data augmentation depicts horizontal flip with a 50%. Images can be horizontally flipped with a 50% probability, which means there's an equal possibility of an image being flipped or not flipped during training and rotating randomly between -30 and 30 degrees. Images can be rotated clockwise or counterclockwise by the specified degree. During data augmentation, rotation and horizontal flip can be used simultaneously. This enhances the dataset's diversity, allowing the model to learn from a wider range of visual variances. Fig. 5 explains the mechanism of increasing data

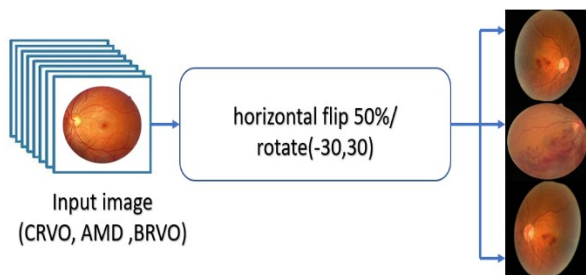


Fig. 5. Image augmentation

C. Model

In our study, we employed the YOLOv8 model, which was obtained through pip and trained using a labeled dataset (Ophthalmic Data). ADAM optimizer was trained with a momentum of 0.937, learning rate of 0.01, batch size of 32, weight decay of 0.0005, and 30 epochs. The results we obtained were sufficient to choose the parameters mentioned above. There are several scaled variants available for YOLOv8, including small, nano, large, medium, and extra-large. For our model, we opted for YOLOv8n-cls, specifically the nano version, due to its compact size, lightweight nature, high speed, and performance. This version comprises 2.7 million parameters and includes 73 layers. The Python 3 language was used in the Google Colab integrated programming environment (Colab Pro). Hardware accelerator type (T4 GPU) for faster computation, allowing for more resource-intensive tasks.

D. Model Evaluation

Since accuracy establishes the classifier's ability to provide a correct diagnosis, the accuracy test was utilized to assess the supplied model. Equation (1) displays the accuracy equation [60].

$$Accuracy = \frac{TP + TN}{TP + TN + FP + FN} \quad (1)$$

Also, Precision, Recall and F1-score were used to measure the performance of our presented model, as these are the most popular and efficient measures in the implementation of models. These measures are explained in the following equations.

$$Precision = \left(\frac{TP}{(TP + FP)} \right) \quad (2)$$

$$Recall = \left(\frac{TP}{(TP + FN)} \right) \quad (3)$$

$$F1 - score = \left(2 \times \frac{(Precision \times Recall)}{(Precision + Recall)} \right) \quad (4)$$

- TP - denotes the number of true positives (The outcome is positive and expected to be positive).
- FN - denotes the number of false negatives (The outcome is positive, but it is predicted to be negative).
- FP - represents the number of false positives (The outcome is negative, and it is expected to be negative).
- TN - represents the number of true negatives (The outcome is negative, but it is predicted to be positive).

V. EXPERIMENT RESULTS

The results show that the proposed method is feasible and effective in classifying and detecting eye diseases. The greatest accuracy value in Speed: 0.2 ms inference, 0.1 ms preprocess, 0.0 ms loss, and 0.0 ms postprocess per image. The ideal time during 30 epochs was 0.6 hours achieved an accuracy rate of 94%, the Precision was 96.2%, recall was 96.6%, the f1 was 96.3% At a time of 0.6 hours was achieved by training the model on the Ophthalmic dataset. The highest category among the categories was BRVO accuracy was achieved 100%, as the number of test images was 110 images,

all of which were correctly classified as BRVO followed by the two categories DR, CRVO which achieved a high accuracy rate of 99%, while the lowest of the seven categories was glaucoma which achieved an accuracy rate of 87%. Out of a total of 216 images, he incorrectly classified 29 images, six of which were predicted to be cataracts, while 23 images were predicted to be a healthy condition. This indicates that there is a very large similarity in features between the healthy condition and glaucoma. This increased the difficulty of training the model, requiring more images to compensate Differences in each picture. The Fig. 5 shows the confusion matrix of the number of images for each category, and the ability of the proposed model to predict the images, while the Fig. 6 shows input features with varying ranges may be normalized to a standard scale This makes it easier to understand and obtain accuracy for each of the seven categories.

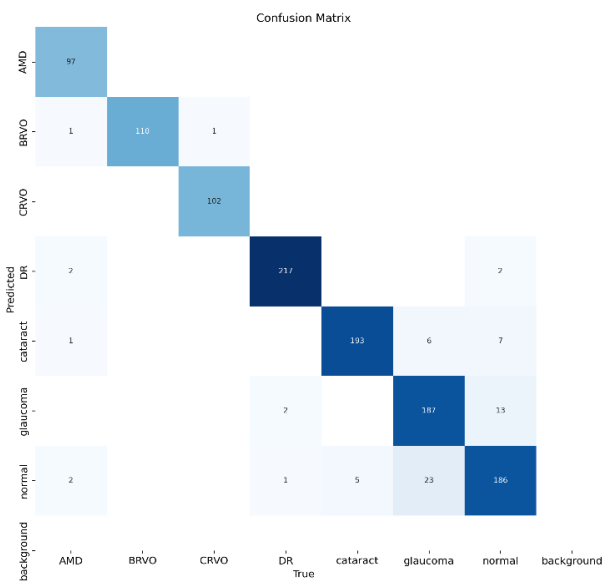


Fig. 6. Confusion Matrix on the test data

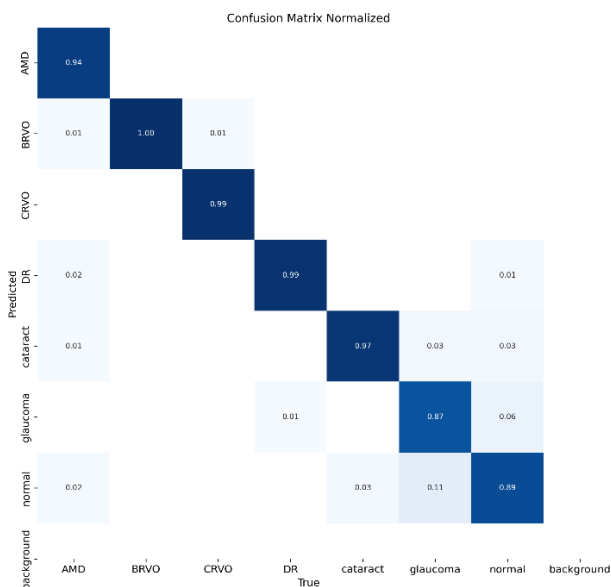


Fig. 7. Confusion matrix on the test data normalized

The proposed model was presented and its effectiveness in classifying eye diseases was compared with previous studies that use the same categories used in our research. It is close to our research in terms of using traditional CNN models and the number of categories used. The comparison is shown in the table. The results indicate that compared to the first study in the Table II, our research greatly excels in terms of the number of images as well as the number of classified categories, in addition to the major challenge is accuracy. We can say that the architecture or construction of the CNN requires training the model from the beginning, and this is the opposite of the model used, which is fast, lightweight, and does not require a lot of storage space. Compared to other studies, it achieved a high accuracy rate. Table II shows comparison between previous studies.

TABLE II. COMPARISON BETWEEN PREVIOUS STUDIES

Model	Time during training	Total parameters	Accuracy
Vgg16	2.1 (H)	138.4m	88%
Resnet50	1.4 (H)	25.6m	92%
YOLOv8n-cls	0.6 (H)	2.7m	94%

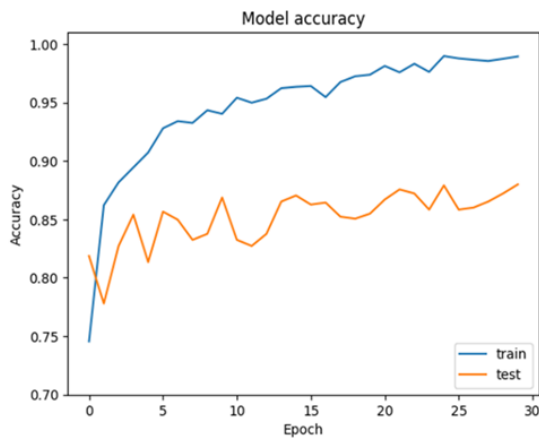
When compared with the model conventional models like VGG16 and Resnet50 are two popular convolutional neural network (CNN) architectures widely used in computer vision tasks, particularly image classification. The aforementioned models were trained on the same data (Ophthalmic Data) in addition to the same parameters chosen for the YOLOv8 model in terms of batch size, image size, number of epochs, and optimizer. where resnet50 got an accuracy of 92%. In an estimated time of 1.4 hours and Vgg16 got 88%. In an estimated time of 2.1 hours as as illustrated in Table III. In addition, the proposed model is characterized by simple mathematical operations by containing 2.7 million parameters, compared to resnet50, which contains 25.6 million parameters Size up to 98 (MB), as well as vgg16, which contains 138.4 million parameters Size up to 528 (MB). This indicates the presence of complex mathematical operations during the classification process, which may require large storage spaces.

TABLE III. COMPARE YOLO WITH RESNET50 AND VGG16

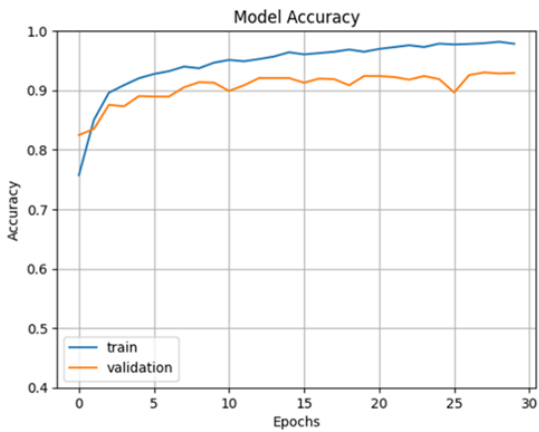
S.N	Paper	Pixel image	No. of Images	No. of Classes	Accuracy
1	[49]	224×224	1,748	5	81%
2	[62]	224×224	4200	4	94%
3	[60]	700×500	224	4	88.4%
4	Proposed Model	224×224	5787	7	94%

An accuracy comparison of the three models with respect to the epoch number is presented for the training and testing processes are in Fig. 8(a), Fig. 8(b), and Fig. 8(c).

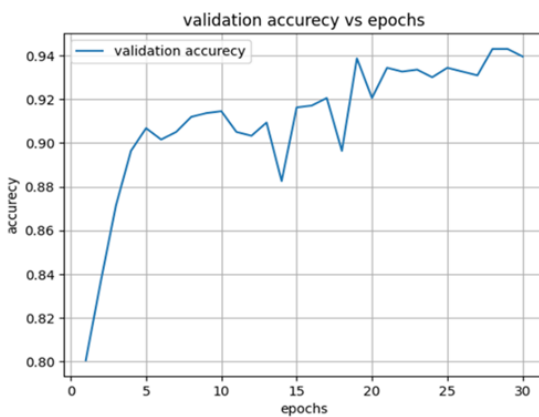
The Fig. 9 Top-5 accuracy is determined by checking whether the correct (ground truth) class is among the top five predictions. If the correct class is among the top five, the prediction is considered correct.



(a) Vgg16 accuracy rate



(b) Resnat50 accuracy rate



(c) YOLOv8 accuracy rate

Fig. 8. Accuracy comparison of the three models with respect to the epoch number



Fig. 9. Top 5 Accuracy some of AMd, CRVO, Cataract and Glaucoma

VI. CONCLUSION

Eye diseases pose a significant challenge in causing blindness, representing irreversible conditions. However, early detection increases the likelihood of successful treatment. In this study, we employed YOLOv8 to classify prominent eye diseases. The selected model, YOLOv8n-cls, was trained on a dataset named (Ophthalmic data) from three different sources (Roboflow, Kaggle and Medical Clinics) which contains 5787 fundus image. The achieved results demonstrated remarkable accuracy, with a 94% accuracy rate, the Precision was 96.2%, recall was 96.6%, the f1 was 96.3%. attained in just 30 epochs. These effective results can help doctors decide to detect these diseases early and avoid the risk of blindness. These findings highlight that the chosen model strikes a balance between accuracy, size and time. This observation holds true, particularly when compared to training vgg16 and Resnet50 models on the same dataset with identical parameters, where YOLO outperformed the mentioned models. Although there are many limitations and obstacles to medical applications, the most important of which is the data set, which is considered a critical component that directly influences the performance, generalization, and robustness of deep learning models. This is why it is difficult to obtain a comprehensive database that contains a larger number of categories. We faced difficulty in the stage of data collection and diagnosis by doctors due to time constraints. We were able to classify six diseases, which are considered the most well-known diseases. Future work will focus on collecting more data to train the model and extract features that avoid misclassification. More categories for example. Arteriosclerotic retinopathy (AR), retinal artery occlusion (BRAO), Hemi-Central Retinal Vein Occlusion and etc. In addition to features to improve classification accuracy.

REFERENCES

- [1] World Health Organization, *Blindness and vision impairment*. World Health Organization, 2023, <https://www.who.int/news-room/factsheets/detail/blindness-and-visual-impairment>.
- [2] X. Luo, J. Li, M. Chen, X. Yang, and X. Li, "Ophthalmic disease detection via deep learning with a novel mixture loss function," *IEEE Journal of Biomedical and Health Informatics*, vol. 25, no. 9, pp. 3332-3339, 2021, doi: 10.1109/JBHI.2021.3083605.
- [3] A.K. Bitto, M. H. Bijoy, M. S. Arman, I. Mahmud, A. Das, and J. Majumder, "Sentiment analysis from Bangladeshi food delivery startup based on user reviews using machine learning and deep learning," *Bulletin of Electrical Engineering and Informatics*, vol. 12, no. 4, pp. 2282-2291, 2023, doi: 10.11591/eei.v12i4.4135.
- [4] E. Valeriani *et al.*, "Antithrombotic treatment for retinal vein occlusion: a systematic review and meta-analysis," *Journal of Thrombosis and Haemostasis*, vol. 21, no. 2, pp. 284-293, 2023, doi: 10.1016/j.jth.2022.10.003.
- [5] J. H. Wu, T. Nishida, R. N. Weinreb, and J. W. Lin, "Performances of machine learning in detecting glaucoma using fundus and retinal optical coherence tomography images: a meta-analysis," *American Journal of Ophthalmology*, vol. 237, pp. 1-12, 2022, doi: 10.1016/j.ajo.2021.12.008.
- [6] A. Aslam, S. Farhan, M. A. Khaliq, F. Anjum, A. Afzaal, and F. Kanwal, "Convolutional Neural Network-Based Classification of Multiple Retinal Diseases Using Fundus Images," *Intelligent Automation & Soft Computing*, vol. 36, no. 3, pp. 2607-2622, 2023, doi: 10.3390/bioengineering10010025.
- [7] A. Misra, H. Gopalan, R. Jayawardena, A. P. Hills, M. Soares, A. A. Reza-Albarrán, and K. L. Ramaiya, "Diabetes in developing

- countries," *Journal of Diabetes*, vol. 11, no.7, pp. 522-539, 2019, doi: 10.1111/1753-0407.12913.
- [8] R. Pradeep and V. Mohan, "Epidemiology of type 2 diabetes in India," *Indian journal of ophthalmology*, vol. 69, no. 11, 2932, 2021, doi: 10.4103/ijo.IJO_1627_21.
- [9] Y. Liang, M. Li, Y. Yang, L. Qiao, H. Xu, and B. Guo, "pH/glucose dual responsive metformin release hydrogel dressings with adhesion and self-healing via dual-dynamic bonding for athletic diabetic foot wound healing," *ACS nano*, vol. 16, no. 2, pp. 3194-3207, 2022, doi: 10.1021/acsnano.1c11040.
- [10] J. C. Chan *et al.*, "The lancet Commission on diabetes: using data to transform diabetes care and patient lives," *The Lancet*, vol. 396, no. 10267, pp. 2019-2082, 2020, doi: 10.1016/S0140-6736(20)32374-6.
- [11] X. Lin *et al.*, "Global, regional, and national burden and trend of diabetes in 195 countries and territories: an analysis from 1990 to 2025," *Scientific reports*, vol. 10, no. 1, p. 14790, 2020, doi: 10.1038/s41598-020-71908-9.
- [12] C. K. Sen, "Human wound and its burden: updated 2020 compendium of estimates," *Advances in wound care*, vol. 10, no. 5, pp. 281-292, 2021, doi: 10.1089/wound.2021.0026.
- [13] L. Wang *et al.*, "Prevalence and treatment of diabetes in China, 2013-2018," *Jama*, vol. 326, no. 24, pp. 2498-2506, 2021, doi: 10.1001/jama.2021.22208.
- [14] Y. Zheng, S. H. Ley, and F. B. Hu, "Global aetiology and epidemiology of type 2 diabetes mellitus and its complications," *Nature reviews endocrinology*, vol. 14, no. 2, pp. 88-98, 2018, doi: 10.1038/nrendo.2017.151.
- [15] S. Dutta, B. Manideep, S. M. Basha, R. D. Caytiles, and N. Iyengar, "Classification of diabetic retinopathy images by using deep learning models," *International Journal of Grid and Distributed Computing*, vol. 11, no. 1, pp. 89-106, 2018, doi: 10.14257/ijgcd.2018.11.1.09.
- [16] A. D. Bhatwadekar, A. Shughoury, A. Belamkar, and T. A. Ciulla, "Genetics of diabetic retinopathy, a leading cause of irreversible blindness in the industrialized world," *Genes*, vol. 12, no. 8, p. 1200, 2021, doi: 10.3390/genes12081200.
- [17] I. S. Forrest *et al.*, "Genome-wide polygenic risk score for retinopathy of type 2 diabetes," *Human Molecular Genetics*, vol. 30, no. 10, pp. 952-960, 2021, doi: 10.1093/hmg/ddab067.
- [18] A. Qassim, E. Souzeau, G. Hollitt, M. M. Hassall, O. M. Siggs, and J. E. Craig, "Risk stratification and clinical utility of polygenic risk scores in ophthalmology," *Translational Vision Science & Technology*, vol. 10, no. 6, pp. 14-14, 2021, doi: 10.1167/tvst.10.6.14.
- [19] L. Nicholson, S. J. Talks, W. Amoaku, K. Talks, and S. Sivaprasad, "Retinal vein occlusion (RVO) guideline: executive summary," *Eye*, vol. 36, no. 5, pp. 909-912, 2022, doi: 10.1038/s41433-022-02007-4.
- [20] E. Valeriani *et al.*, "Antithrombotic treatment for retinal vein occlusion: a systematic review and meta-analysis," *Journal of Thrombosis and Haemostasis*, vol. 21, no. 2, pp. 284-293, 2023, doi: 10.1016/j.jth.2022.10.003.
- [21] D. Nagasato *et al.*, "Automated detection of a nonperfusion area caused by retinal vein occlusion in optical coherence tomography angiography images using deep learning," *PLoS one*, vol. 14, no. 11, p. e0223965, 2019, doi: 10.1371/journal.pone.0223965.
- [22] R. Aggarwal *et al.*, "Diagnostic accuracy of deep learning in medical imaging: a systematic review and meta-analysis," *NPJ digital medicine*, vol. 4, no. 1, 2021, doi: 10.1038/s41746-021-00438-z.
- [23] P. K. Mall *et al.*, "A comprehensive review of deep neural networks for medical image processing: Recent developments and future opportunities," *Healthcare Analytics*, vol. 4, no. 1, p. 100216, 2023, doi: 10.1016/j.health.2023.100216.
- [24] Q. Chen *et al.*, "Artificial intelligence can assist with diagnosing retinal vein occlusion," *International Journal of Ophthalmology*, vol. 14, no. 12, pp. 1895-1902, 2021, doi: 10.18240/ijo.2021.12.13.
- [25] D. Yang *et al.*, "Deep learning in optical coherence tomography angiography: Current progress, challenges, and future directions," *Diagnostics*, vol. 13, no. 2, 2023, doi: 10.3390/diagnostics13020326.
- [26] A. L. Rothman, A. S. Thomas, K. Khan, and S. Fekrat, "Central retinal vein occlusion in young individuals: a comparison of risk factors and clinical outcomes," *Retina*, vol. 39, no. 10, pp. 1917-1924, 2019, doi: 10.1097/LAE.0000000000002278.
- [27] S. S. Hayreh, "Photocoagulation for retinal vein occlusion," *Progress in retinal and eye research*, vol. 85, p. 100964, 2021, doi: 10.1016/j.preteyeres.2021.100964.
- [28] X. T. Zhang *et al.*, "Clinical features of central retinal vein occlusion in young patients," *Ophthalmology and Therapy*, vol. 11, no. 4, pp. 1409-1422, 2022, doi: 10.1007/s40123-022-00534-7.
- [29] Y. Tang, Y. Cheng, S. Wang, Y. Wang, P. Liu, and H. Wu, "The development of risk factors and cytokines in retinal vein occlusion," *Frontiers in Medicine*, vol. 9, p. 910600, 2022, doi: 10.3389/fmed.2022.910600.
- [30] D. Nagasato *et al.*, "Deep neural network-based method for detecting central retinal vein occlusion using ultrawide-field fundus ophthalmoscopy," *Journal of ophthalmology*, vol. 1, 2018, doi: 10.1155/2018/1875431.
- [31] J. P. Li *et al.*, "Digital technology, tele-medicine and artificial intelligence in ophthalmology: A global perspective," *Progress in retinal and eye research*, vol. 82, p. 100900, 2021, doi: 10.1016/j.preteyeres.2020.100900.
- [32] L. P. Cen *et al.*, "Automatic detection of 39 fundus diseases and conditions in retinal photographs using deep neural networks," *Nature communications*, vol. 12, no. 1, p. 4828, 2021, doi: 10.1038/s41467-021-25138-w.
- [33] J. Xu, K. Xue, and K. Zhang, "Current status and future trends of clinical diagnoses via image-based deep learning," *Theranostics*, vol. 9, no. 25, p. 7556, 2019, doi: 10.7150/thno.38065.
- [34] M. M. Butt, D. A. Iskandar, S. E. Abdelhamid, G. Latif, and R. Alghazo, "Diabetic retinopathy detection from fundus images of the eye using hybrid deep learning features," *Diagnostics*, vol. 12, no. 7, p. 1607, 2022, doi: 10.3390/diagnostics12071607.
- [35] S. Jabbehdari, G. Yazdanpanah, L. B. Cantor, and A. R. Hajrasouliha, "A narrative review on the association of high intraocular pressure and glaucoma in patients with retinal vein occlusion," *Annals of Translational Medicine*, vol. 10, no. 19, p. 1072, 2022, doi: 10.21037/atm-22-2730.
- [36] Y. B. Kim, C. H. Lee, Y. K. Shin, S. E. Kyung, and Y. S. Seo, "Early retinal hemorrhage absorption rate and long term clinical outcomes in branch retinal vein occlusion," *Journal of the Korean Ophthalmological Society*, vol. 62, no. 4, pp. 496-506, 2021.
- [37] S. C. Akdemir and B. O. Gunay, "Comparison of anti-VEGF results between non-ischemic branch retinal vein occlusion and ischemic branch retinal vein occlusion with early sector panretinal photocoagulation," *Journal Français 'Ophthalmologie*, vol. 45, no. 9, pp. 1042-1047, 2022, doi: 10.1016/j.jfo.2022.03.014.
- [38] J. Miao *et al.*, "Deep learning models for segmenting non-perfusion area of color fundus photographs in patients with branch retinal vein occlusion," *Frontiers in Medicine*, vol. 9, p. 794045, 2022, doi: 10.3389/fmed.2022.794045.
- [39] Y. Ji, Y. Ji, Y. Liu, Y. Zhao, and L. Zhang, "Research progress on diagnosing retinal vascular diseases based on artificial intelligence and fundus images," *Frontiers in Cell and Developmental Biology*, vol. 11, p. 1168327, 2023, doi: 10.3389/fcell.2023.1168327.
- [40] I. Weni, P. E. Utomo, B. F. Hutabarat, and M. Alfalah, "Detection of cataract based on image features using convolutional neural networks," *Indonesian Journal of Computing and Cybernetics Systems*, vol. 15, no. 1, pp. 75-86, 2021, doi: 10.22146/ijccs.61882.
- [41] S. H. Heruye *et al.*, "Opere, Current trends in the pharmacotherapy of cataracts," *Pharmaceuticals*, vol. 13, no. 1, 2020, doi: 10.3390/ph13010015.
- [42] Y. Elloumi, "Cataract grading method based on deep convolutional neural networks and stacking ensemble learning," *International Journal of Imaging Systems and Technology*, vol. 32, no. 3, pp. 798-814, 2022, doi: 10.1002/ima.22722.
- [43] J. Wang *et al.*, "A transformer-based knowledge distillation network for cortical cataract grading," *IEEE Transactions on Medical Imaging*, 2023, doi: 10.1109/TMI.2023.3327274.
- [44] S. Serte and A. Serener, "A generalized deep learning model for glaucoma detection," in *2019 3rd International symposium on multidisciplinary studies and innovative technologies (ISMSIT)*, pp. 1-5, 2019, doi: 10.1109/ISMSIT.2019.8932753.
- [45] S. Sotoudeh-Paima, A. Jodeiri, F. Hajizadeh, and H. Soltanian-Zadeh, "Multi-scale convolutional neural network for automated AMD classification using retinal OCT images," *Computers in biology and*

- medicine*, vol. 144, pp. 105368, 2022, doi: 10.1016/j.compbimed.2022.105368.
- [46] A. Thomas, P. Harikrishnan, A. K. Krishna, P. Palanisamy, and V. P. Gopi, "A novel multiscale convolutional neural network based age-related macular degeneration detection using OCT images," *Biomedical Signal Processing and Control*, vol. 67, p. 102538, 2021, doi: 10.1016/j.cmpb.2021.106294.
- [47] M. H. Najim, S. K. Abdulateef, and A. H. Alasadi, "Early detection of tomato leaf diseases based on deep learning techniques," *International Journal of Artificial Intelligence (IJ-AI)*, vol. 13, no. 1, pp. 509-515, 2023, doi: 10.11591/ijai.v13.i1.pp509-515.
- [48] S. Sengupta *et al.*, "A review of deep learning with special emphasis on architectures, applications and recent trends," *Knowledge-Based Systems*, vol. 194, p. 105596, 2020, doi: 10.1016/j.knsys.2020.105596.
- [49] R. Sarki, K. Ahmed, H. Wang, Y. Zhang, and K. Wang, "Convolutional neural network for multi-class classification of diabetic eye disease," *EAI Endorsed Transactions on Scalable Information Systems*, vol. 9, no. 4, 2021, doi: 10.4108/eai.16-12-2021.172436.
- [50] A. Ali *et al.*, "Machine learning based automated segmentation and hybrid feature analysis for diabetic retinopathy classification using fundus image," *Entropy*, vol. 22, no. 5, p. 567, 2020, doi: 10.3390/e22050567.
- [51] R. Narlan and E. P. Widiyanto, "Automated pavement defect detection using YOLOv8 object detection algorithm," *Prosiding KRTJ HPJI*, vol. 16, no. 1, pp. 1-13, 2023, doi: 10.58674/phpi.v16i1.388.
- [52] G. G. Casas, Z. H. Ismail, M. M. Limeira, A. A. da Silva, and H. G. Leite, "Automatic detection and counting of stacked eucalypt timber using the YOLOv8 model," *Forests*, vol. 14, no. 12, p. 2369, 2023, doi: 10.3390/f14122369.
- [53] F. Khan, N. Zafar, M. N. Tahir, M. Aqib, H. Waheed, and Z. A. Haroon, "Mobile-based system for maize plant leaf disease detection and classification using deep learning," *Frontiers in Plant Science*, vol. 14, p. 1079366, 2023, doi: 10.3389/fpls.2023.1079366.
- [54] A. Inui *et al.*, "Detection of elbow OCD in the ultrasound image by artificial intelligence using YOLOv8," *Applied Sciences*, vol. 13, no.13, 2023, doi: 10.3390/app13137623.
- [55] M. Alruwaili *et al.*, "Deep Learning-Based YOLO Models for the Detection of People With Disabilities," in *IEEE Access*, vol. 12, pp. 2543-2566, 2024, doi: 10.1109/ACCESS.2023.3347169.
- [56] G. Jocher, A. Chaurasia, and J. Qiu, "YOLO by Ultralytics," URL: <https://github.com/ultralytics/ultralytics>, 2023.
- [57] X. Li *et al.*, "Generalized focal loss: Learning qualified and distributed bounding boxes for dense object detection," *Advances in Neural Information Processing Systems*, vol. 33, pp. 21002-21012, 2020.
- [58] X. Wang, H. Li, X. Yue, and L. Meng, "A comprehensive survey on object detection YOLO," *Proceedings http://ceur-ws.org ISSN*, vol. 1613, p. 0073, 2023.
- [59] S. Dash, J. Supraja, D. Vanshitha, C. Keerthi, and E. Dinesh, "Retinal Disease Prediction Using Deep Learning," *Journal of Engineering Sciences*, vol. 14, no. 7, 2023, doi: 10.3390/jimaging9040084.
- [60] E. Abitbol *et al.*, "Deep learning-based classification of retinal vascular diseases using ultra-widefield colour fundus photographs," *BMJ Open Ophthalmology*, vol. 7, no. 1, p. e000924, 2022, doi: 10.1136/bmjophth-2021-000924.
- [61] W. Xu, Z. Yan, N. Chen, Y. Luo, Y. Ji, M. Wang, and Z. Zhang, "Development and application of an intelligent diagnosis system for retinal vein occlusion based on deep learning," *Disease Markers*, vol. 2022, 2022, doi: 10.1155/2022/4988256.
- [62] T. Babaqi, M. Jaradat, A. E. Yildirim, S. H. Al-Nimer, and D. Won, "Eye disease classification using deep learning techniques," *arXiv preprint arXiv: 2307.10501*, 2023, doi: 10.48550/arXiv.2307.10501.
- [63] C. Wan, R. Hua, K. Li, X. Hong, D. Fang, and W. Yang, "Automatic diagnosis of different types of retinal vein occlusion based on fundus images," *International Journal of Intelligent Systems*, vol. 2023, 2022, doi: 10.1155/2023/1587410.
- [64] S. K. Abdulateef, A. N. Ismael, M. D. Salman, "Feature weighting for parkinson's identification using single hidden layer neural network," *International Journal of Computing*, vol. 22, no. 2, pp. 225-230, 2022, doi: 10.47839/ijc.22.2.3092.